

# Orbital-selective charge dynamics in $\text{YTiO}_3$ across the magnetic transition: Combined local-density approximation and dynamical mean-field theory

L. Craco,<sup>1</sup> S. Leoni,<sup>1</sup> M. S. Laad,<sup>2</sup> and H. Rosner<sup>1</sup><sup>1</sup>Max-Planck-Institut für Chemische Physik fester Stoffe, 01187 Dresden, Germany<sup>2</sup>Max-Planck-Institut für Physik Komplexer Systeme, 01187 Dresden, Germany

(Received 11 July 2007; published 26 September 2007)

The orbital-selective nature of charge dynamics in transition-metal oxides is an ill-understood phenomenon in general. Understanding its evolution across an orbital and/or magnetic phase transition promises to shed light upon the nature of ordering in strongly correlated systems. Motivated by recent work probing changes in optical absorption across the paramagnetic-ferromagnetic transition in  $\text{YTiO}_3$ , we study this issue within LDA+DMFT. We obtain good agreement with experiment, showing appreciable changes across the magnetic transition. Our study thus constitutes an attempt to address this outstanding issue and should be widely applicable to other oxides of great interest.

DOI: [10.1103/PhysRevB.76.115128](https://doi.org/10.1103/PhysRevB.76.115128)

PACS number(s): 71.27.+a, 71.30.+h, 72.80.Ga, 78.30.Ly

Multiorbital correlations in transition-metal oxides are recognized to be important toward consistent understanding of their physical responses.<sup>1</sup> Their complex and fascinating responses require an understanding in terms of the competition between local (Hubbard parameters, crystal-field symmetry, and spin-orbit coupling) and itinerant aspects.<sup>2</sup> Titanium based oxides have been intensively studied in this context.<sup>1</sup> They are attractive because one may view them as the electron analog ( $3d^1$ ) of the famous cuprates ( $3d^9$ ). Further, Jahn-Teller distortions are expected to play a significantly reduced role in the  $t_{2g}$  sector, making carrier localization (self-trapping) harder to achieve. On the other hand, strongly anisotropic hopping, in conjunction with strong multiorbital correlations, tends to favor localization, and the actual outcome of these competing tendencies is a very complex theoretical problem to solve.<sup>1,2</sup>

The nature of charge dynamics in a multiorbital (MO) system has turned out to be much more interesting than anticipated, even within the  $d=\infty$  Hubbard model framework. In a transition-metal oxide (TMO), MO-Hartree shifts in concert with large spectral weight transfer due to dynamical correlations drive orbital-selective (OS) Mott transitions.<sup>3,4</sup> New non-Fermi liquid metallic states emerge as a result; this is out of scope of a one-band Hubbard model in  $d=\infty$ , where collective Kondo screening results in a correlated Fermi Liquid metal for  $T < T_{coh}$ ,<sup>1</sup> a lattice coherence scale associated with the collective Kondo effect at each lattice site. Hitherto, these fascinating phenomena have been investigated for paramagnetic Mott transitions.<sup>3,4</sup> How is this picture affected when the system undergoes a magnetic and/or orbital ordering transition? Understanding the modification of anisotropic charge dynamics in a multiorbital picture across the order-disorder transitions promises to shed light upon the precise nature of the correlation driven phase transitions themselves. Here, we study this issue theoretically.

In this work, we study certain key aspects of the physics of *ferromagnetic* insulating (FI)  $\text{YTiO}_3$ .<sup>5</sup> In the  $3d^1$  configuration, ferromagnetism usually arises from intersite magnetic exchange between *orthogonal* orbitals.<sup>6</sup> Structural details of the real material are crucial in deciding the actual ordered ground state(s) in TMOs. In a perfectly cubic symmetry, for

example, long range magnetic order is ruled out at finite temperatures ( $T$ ) in a model having perfect orbital degeneracy,<sup>7</sup> using an ingenious application of the Mermin-Wagner theorem. Given the finite- $T$  magnetic order found in the perovskite titanates, this implies that any modeling based on perfect  $t_{2g}$  orbital degeneracy<sup>8</sup> is flawed. In titanates, this difficulty is overcome because the real structure has  $\text{GdFeO}_3$  distortions,<sup>9</sup> which removes the  $t_{2g}$  degeneracy and implies orbital order. This is indeed observed experimentally<sup>10,11</sup> in  $\text{YTiO}_3$ , which has antiferro-orbital order (AFOO) in the ground state. In Fig. 1, we show the ground state orbital character obtained from a local spin density approximation (LSDA) calculation in the real structure of  $\text{YTiO}_3$  (see below). Given that the exchange in magnetic insulators is sensitively determined by orbital order setting in well above  $T_c$ , a description of the FI state of  $\text{YTiO}_3$  requires a consistent treatment of these correlations. Indeed, Mochizuki and Imada<sup>12</sup> constructed and solved a multiband Hubbard model, deriving the correct (FI-AFOO) ground state at the Hartree-Fock level. Schmitz *et al.*<sup>13</sup> extended this approach to study magnetic excitations in detail, obtaining good agreement with experiments. Pavarini *et al.*<sup>14</sup> and Craco *et al.*<sup>15</sup> used local-density approximation (LDA)+dynamical mean-field theory (DMFT) for the *paramagnetic* phase of both  $\text{LaTiO}_3$  and  $\text{YTiO}_3$ ; both calculations obtain good agreement with key experiments. Such a calculation for the AFI/FI phases has never been attempted; here, we study the FI phase in  $\text{YTiO}_3$ .

$\text{YTiO}_3$  crystallizes in the distorted cubic perovskite structure.<sup>16</sup> For this structure, scalar-relativistic band-structure calculations have been performed with LSDA. We employ the linear muffin-tin orbital scheme in the atomic sphere approximation, with combined correction terms.<sup>17</sup> Self-consistency is reached by performing calculations on a  $16 \times 16 \times 16$   $\mathbf{k}$  mesh. The radii of the atoms were chosen as  $r=3.1$  (Y) a.u.,  $r=2.06$  (O) a.u., and  $r=2.64$  (Ti) a.u. in order to minimize their overlap. The LSDA calculation performed within this scheme yields three  $t_{2g}$  bands, each about 1.6 eV wide. The orbital occupations resulting therefrom are  $n_a, n_b, n_c=0.31, 0.27, 0.18$  for the majority-spin bands. The one-particle energies are  $\epsilon_a, \epsilon_b, \epsilon_c=0.13, 0.44, 0.45$  eV, im-

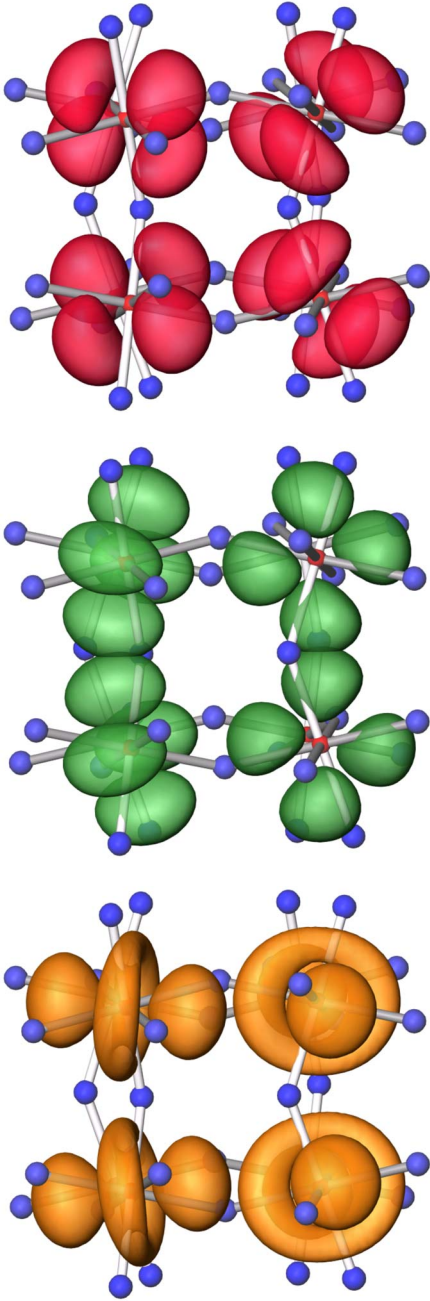


FIG. 1. (Color online)  $t_{2g}$  orbitals in the ferromagnetic state of  $\text{YTiO}_3$ , as obtained within LSDA. Ground state (top/red), first excited state (middle/green), and second excited state (bottom/orange) in the projected  $Pbnm$  primitive cell. The four-sublattice AFOO is clearly shown in the results (see discussion in text). The oxygens are shown in small blue spheres.

plying almost degenerate  $b, c$  orbitals. Since the  $e_g$  density of states (DOS) lies 2.0 eV above the  $t_{2g}$  DOS, we restrict ourselves to the  $t_{2g}$  sector<sup>18</sup> in what follows. Given the partial occupation of each  $t_{2g}$  orbital,  $U, U'$  (defined below) are essential to produce a Mott insulator, and strong  $J_H \approx 1.0$  eV is required to produce ferromagnetism. This mandates the use of a multiorbital Hubbard model, in conjunction with the actual band structure, to describe the physical response of  $\text{YTiO}_3$ .

The Fermi level in Fig. 2 lies very close to a sharp peak in the majority-spin DOS. The minority-spin DOS is gapped close to  $E_F$ . Thus, LSDA does yield the ferromagnetic state: in fact, it yields a half-metallic state. The saturated magnetic moment is found to be  $m=0.76\mu_B/\text{Ti}$ , in nice agreement with the experimental value of  $0.84\mu_B/\text{Ti}$ .<sup>10</sup> Further, the tendency to AFOO is also correctly obtained: the ground state has a staggered orbital order of  $d_a$  and  $d_b$  on neighboring sites in the distorted structure (see Fig. 1). LSDA (LSDA+ $U$ ) underestimates (overestimates) localization, owing to the neglect (replacement) of dynamical correlations by their static forms which neglect quantum fluctuations. The upshot is an incorrect description of spectral weight transfer (SWT), giving rise to large, quantitative disagreement with the experiment.<sup>1,18</sup> These aspects can all be described in a single picture via LDA+DMFT.

Henceforth, we work in orbital basis which diagonalizes the one-particle density matrix in LDA, so that  $G_{ab}^{(0)}(k, \omega) = \delta_{ab}G_{aa}^{(0)}(k, \omega)$ . We introduce the strong, multiorbital correlations by considering a three-orbital Hubbard model for the  $t_{2g}$  sector. The Hamiltonian  $H=H_0+H'$  reads

$$H_0 = \sum_{\mathbf{k}, a, \sigma} \epsilon_{a\sigma}(\mathbf{k}) c_{\mathbf{k}a\sigma}^\dagger c_{\mathbf{k}a\sigma} + \sum_{i, a, \sigma} \epsilon_{a\sigma} n_{ia\sigma}, \quad (1)$$

where  $\epsilon_{a\sigma}(\mathbf{k})$  are the ferromagnetic band dispersions in the LSDA and  $\epsilon_{a\sigma}$  the spin- and orbital-dependent single particle energies. The correlation part is described by

$$H' = U \sum_{i, a} n_{ia\uparrow} n_{ia\downarrow} + U' \sum_{i, a, b} n_{ia} n_{ib} - J_H \sum_{i, a, b} \mathbf{S}_{ia} \cdot \mathbf{S}_{ib}. \quad (2)$$

Here,  $U, U'$  are the intraorbital and interorbital local Coulomb interactions, respectively, and  $J_H$  is the Hund coupling, related by  $U \approx U' + 2J_H$  in the  $t_{2g}$  sector.

To avoid double counting of the (static) mean-field contributions from the electron-electron interactions already included in the LSDA, we employ the strategy used first by Anisimov *et al.*<sup>19</sup> For a multiorbital system with finite  $J_H$ , the one-particle orbital energies are corrected from their LSDA values to  $\epsilon'_{a\sigma} = \epsilon_{a\sigma} - U(n - \frac{1}{2}) + J_H(n_{\sigma} - \frac{1}{2})$ , so that

$$H'_0 = \sum_{\mathbf{k}, a, \sigma} \epsilon_{a\sigma}(\mathbf{k}) c_{\mathbf{k}a, \sigma}^\dagger c_{\mathbf{k}a, \sigma} + \sum_{i, a, \sigma} \epsilon'_{a\sigma} n_{ia\sigma}. \quad (3)$$

We solve  $H=H'_0+H'$  at  $T=0$  for the ferromagnetic phase within LSDA+DMFT, where the MO-DMFT used earlier<sup>15</sup> is extended to treat FM order. We use the multiorbital iterated perturbation theory (MO-IPT) as the impurity solver; this has been shown to be quantitatively accurate for band fillings  $n \leq 1$ .<sup>18</sup> Other choices for the multiorbital impurity solver are either prohibitively costly (such as dynamical DMRG<sup>20</sup> and/or numerical renormalization group<sup>21</sup>) or are restricted to rather high [ $T \gg T_C = 27$  K (Ref. 22)] temperatures [quantum Monte Carlo (QMC)]. Only multiorbital IPT and the noncrossing approximation,<sup>23</sup> along with continuous-time QMC,<sup>24</sup> can access the low- $T$  phase(s). Of these, MO-IPT and non-crossing approximation are numerically extremely fast and efficient solvers and are known to yield the correct low- $T$  physics for the asymmetric Anderson impurity model. Given this situation, we opt for using MO-IPT as an

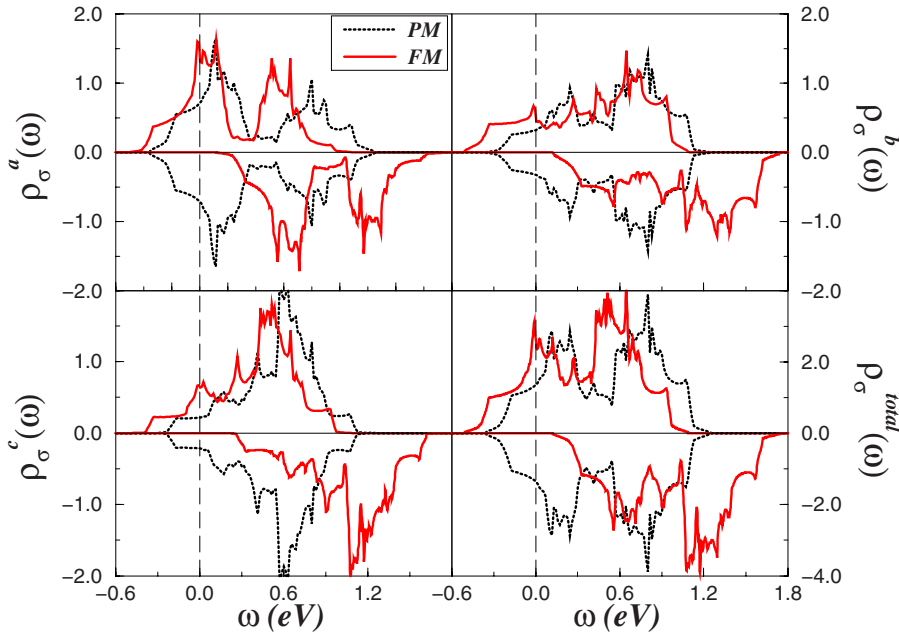


FIG. 2. (Color online) L(S)DA spin- and orbital-resolved  $t_{2g}$  DOSs (first three panels) for both phases: paramagnetic (Ref. 15) (dotted line) and ferromagnetic (solid line). The total DOS is shown in the last panel. All curves have been normalized to unity.

impurity solver for our problem: it has been shown to work quantitatively accurately also for ferromagnetic systems<sup>25,26</sup> treated within the LDA+DMFT scheme.

For the FI-YTiO<sub>3</sub>, this implies separately solving the multiorbital (matrix) DMFT equations for each spin, using the corresponding LSDA DOS as inputs.<sup>25</sup> Generically, MO-DMFT causes a two-step renormalization: (i) it introduces multiorbital Hartree shifts, causing *static* renormalization of crystal-field splittings, etc., and (ii) more importantly, it drives large spin- and orbital-dependent changes in dynamical SWTs in response to small changes in these L(S)DA parameters. In correlated systems, this is crucial for a quantitative description and for describing SWT driven phase transitions, which are inaccessible by less sophisticated techniques.

From LSDA+DMFT, we obtain the fully dressed crystal-field splittings, orbital occupations, spin values, and the full one-particle Green's functions: this enables an exact study of the photoemission spectroscopy (PES), x-ray absorption spectroscopy (XAS), and optical response. Comparison with spectroscopic and optical data is a stringent test of the quality of LSDA+DMFT. Our strategy in what follows is to (i) show how LSDA+DMFT yields good agreement with optical data and (ii) use this to show how OS charge dynamics in a multiorbital system changes across a magnetic phase transition. In the FI phase, we employ the MO-IPT scheme<sup>25</sup> only for the majority-spin channel, the minority one is treated on the Hartree level. Similar to LDA+multiorbital Hartree calculations, the minority bands are shifted to higher energies ( $\omega \geq 2.54$  eV) and, therefore, do not contribute for the many-particle DOS up to these energies within LSDA+DMFT (see discussion below). Hence, we restrict ourselves to treating dynamical correlations in the  $t_{2g}\uparrow$  sector: whether this is a reasonable approximation will depend upon whether the LSDA+DMFT results obtained therefrom give a sufficiently good account of observed spectra up to energies  $O(2.0)$  eV. We will indeed find, *a posteriori*, that this turns out to be true, justifying this approximation.

We now present our results. We choose  $U=4.75$  eV and  $J_H=1.0$  eV, with  $U'=U-2J_H=2.75$  eV, for the ferromagnetic case. While Anisimov *et al.* find a  $U=4.0$  eV from a random-phase approximation screening analysis within the LDA, LDA+DMFT works use  $U=5.0$  eV. We choose  $U=4.75$  eV for the following reason: the treatment of dynamical screening within a constrained LDA generically *overestimates* the reduction of  $U$  by about 20%.<sup>4</sup> This is because the electrons causing the screening are actually themselves correlated, and their screening effect would be less than that caused by totally uncorrelated electrons (as in LDA). With an LSDA bandwidth of 1.6 eV for each orbital ( $a, b, c$  above), the generation of a Mott-Hubbard insulator requires a strong  $U'$ . As seen in solid (red) lines of Fig. 3, the Mott gaps are orbital dependent: the maximally occupied orbital,  $a$ , has the largest Mott-Hubbard gap 0.8 eV, while the higher lying orbitals  $b, c$  have smaller gaps of 0.7 and 0.6 eV, respectively. Strong dynamical SWT from low to high energies drastically modifies the LSDA spectra. Considerable interorbital charge transfer (CT) is also clearly seen: the orbital occupations for the majority-spin channel now are  $n_a, n_b, n_c = 0.39, 0.29, 0.09$ , implying a large CT from the highest orbital ( $c$ ) to the two lower ( $a, b$ ) orbitals—notice the very small weight in  $\rho_c$  compared to  $\rho_{a,b}$  in Fig. 3. Further, this large interorbital CT modifies the local orbital assignment: the orbital  $c$  with energy  $\epsilon_c=0.45$  eV (in LSDA) now lies highest ( $\epsilon'_c=1.04$  eV), followed by  $a$  (in LSDA) which now has energy  $\epsilon'_a=0.84$  eV and by  $b$ , with energy  $\epsilon'_b=0.68$  eV. From the renormalized LDA+DMFT spectral functions, we estimate<sup>27</sup> that the magnetization increases by about 6%, to  $m \approx 0.8\mu_B/\text{Ti}$ , in closer agreement with the measured value of  $0.84\mu_B/\text{Ti}$ . Given the sensitivity of dynamical spectral weight transfer (within DMFT) to changes in the bare one-electron (LSDA) energy scales, we expect that the specific orbital-selective changes in the optical line shapes in different polarizations across  $T_C$  would represent a fingerprint of changes in the *correlated* electronic structure across the ferro-para phase transition. Remarkably, these indeed turn

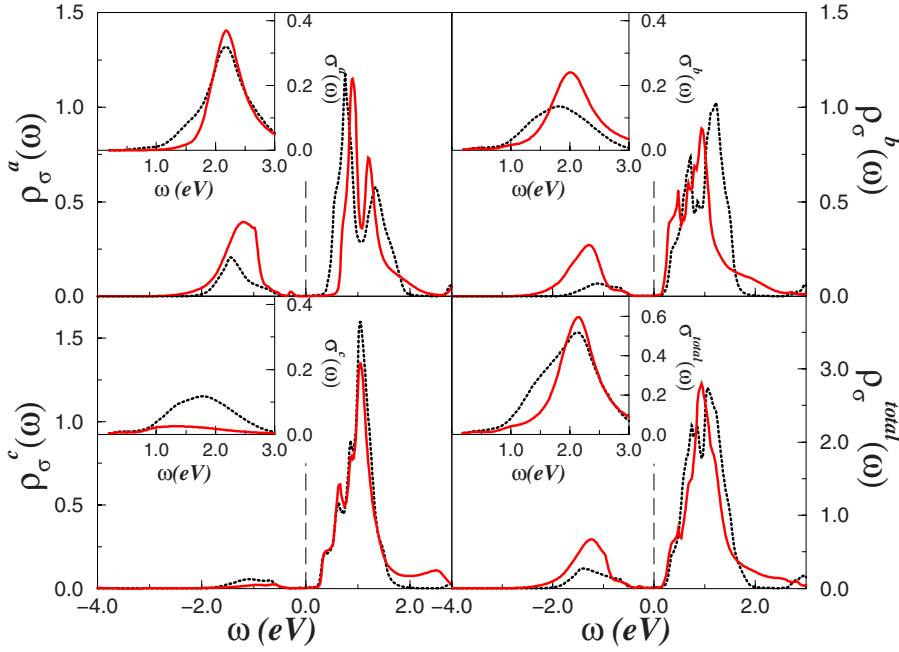


FIG. 3. (Color online) L(S)DA+DMFT spin- and orbital-resolved  $t_{2g}$  DOSs: paramagnetic phase (Ref. 15) (dotted line,  $U=5.0$  eV) and ferromagnetic phase (solid line,  $U=4.75$  eV). The insets show the computed orbital-resolved and total optical conductivities for the PI (Ref. 15) (dotted) and FI (solid) phases. In the FI phase, only the majority channel is shown.

out to be in nice agreement with experiment, as we will indeed find below.

Optical conductivity for the FI state in  $\text{YTiO}_3$  has already been measured.<sup>28,29</sup> These studies reveal several interesting features. (i) The anisotropy of orbital-resolved optical spectra is a fingerprint of the underlying MO dynamical correlations in this material. (ii) Low-energy features arising from transitions to higher crystal-field split states are also seen in the spectra. In particular, the  $T$ -dependent optical spectra show that, as the sample is cooled below  $T_C \approx 27$  K, the dynamical spectral weight is transferred from lower to higher energies in  $a, b$  polarization, while only a *decrease* in the optical weight is seen in the  $c$  polarization. Additionally, weak features around  $\omega_1 \approx 0.4$  eV and  $\omega_2 \approx 0.8$  eV are also visible<sup>29</sup> below the intense high-energy feature centered around  $\omega_h \approx 2.0$  eV in the  $a, b$  polarizations (but not in  $c$  polarization for the FI state<sup>28</sup>). These changes are a fingerprint of how magnetic and orbital orders affect orbital-selective charge dynamics in a MO-Mott system.

In  $d=\infty$ , knowledge of the full matrix propagators,  $G_{ab}(k, \omega)$ , allows one to compute the optical conductivity without any further approximation. This is because vertex corrections entering the Bethe-Salpeter equations for the ac conductivity vanish in  $d=\infty$ .<sup>30</sup> This can be extended to our multiorbital case because  $G_{ab}(k, \omega) = \delta_{ab} G_{aa}(k, \omega)$ .<sup>31,32</sup> Earlier work has discussed optical spectra for the paramagnetic (high- $T$ ) case. We have extended these works to compute the orbital-resolved and total optical conductivities for the FI state of  $\text{YTiO}_3$ . Earlier work using MO-IPT for the paramagnetic insulating (PI) case gave very good agreement with published results up to 2.0 eV.<sup>15</sup> The results of Ref. 15 are shown by the dashed (black) line in the insets of Fig. 3. Results for the FI state are shown by solid (red) lines. Basically, all features found in experiment<sup>28</sup> are faithfully reproduced by MO-DMFT (IPT). Further, the spectra do show the following striking features vis-a-vis experiment:

(i) The overall line shapes in different polarizations re-

main qualitatively unaffected up to 2.0 eV, as observed experimentally.

(ii) The redistribution of optical spectral weight among different  $t_{2g}$  orbitals across the FI-PI phase transition is well reproduced by LSDA+DMFT (see inset to Fig. 3). In particular, the transfer of spectral weight from low to high energies in the  $a, b$  polarizations and the uniform decrease in the weight in  $c$  polarization are well reproduced by the theory. The high-energy peak at  $\omega_h \approx 2.0$  eV is now identified with an interorbital Mott-Hubbard excitation ( $U'$ ), while the lower-energy structures (around 0.5–0.8 eV) can be attributed to electronic transitions to the crystal-field excited states (see Fig. 3).

Comparing with experiment,<sup>28</sup> we find that the optical transitions up to 2.0 eV are well described by our LSDA+DMFT. However, we do not observe a higher-energy peak,  $B$ , shown in the experiment. There are a few reasons for this discrepancy. Peak  $B$  could involve transitions between the  $t_{2g}$  and the (higher in energy)  $e_g$  bands:<sup>33</sup> this is out of the scope of our work, which considers only the  $t_{2g}$  bands. Future work should address this issue, but we opine that spin- and orbital-polarized spectroscopy would shed more light on this aspect.

More care might have to be taken while making a detailed theory-experiment comparison. Gössling *et al.*<sup>28</sup> compare their results with the LDA+DMFT work for the paramagnetic phase. They identify the higher-energy peak  $B$  with transitions between the Hubbard bands and argue for a larger value of  $U'$  ( $=3.72$ ) eV as employed by Pavarini *et al.*<sup>31</sup> Using our parameter set, we identify the 2.0 eV peak as arising from transitions between the Hubbard bands. In our opinion, the strength of our approach is that nearly the same parameters give an excellent fit to *both* one-electron (PES) and optical spectroscopies for the PI phase.<sup>15</sup> On the other hand, those used by Pavarini *et al.* result in a much higher onset of absorption features, as one can see by a direct comparison.<sup>15</sup> Since there is no reason to suppose that  $U, U'$  change drastically across the FI-PI transition (both are Mott

insulators), this suggests that the parameters  $U \simeq 4.75$  eV,  $U' \simeq 2.75$  eV,  $J_H = 1.0$  eV might be appropriate for FI-YTiO<sub>3</sub>.

Secondly, Gössling *et al.*<sup>28</sup> attempt to identify peak *A* with an excitonic feature nearly splitted from *B*. This requires introduction of an electron-hole interaction,  $V \simeq 1.0$  eV. While such an effect may exist, the motivation for its introduction is not clear: for example, within DMFT, it should lead to a similar feature in one-particle spectroscopies. It might be worthwhile to see whether associated feature(s) are seen in XAS studies; this could confirm or rule out this possibility.

Our LSDA+DMFT results indicate that peak *A* is associated with incoherent transitions between the interorbital ( $U'$ ) split Hubbard bands and thus lead to a different interpretation from the one invoked by Gössling *et al.*<sup>28</sup> The much weaker lower-energy features are attributable to transitions to the crystal-field split excited states. We find no evidence for dispersing features in different polarizations. This implies suppression of orbital fluctuations at sufficiently low energies below the (Mott) gap in the AFOO phase, as discussed before for titanates in a broader context.<sup>12,13</sup> This is in agree-

ment with earlier LDA+DMFT works,<sup>14,34</sup> as well as with an exact argument,<sup>7</sup> disfavoring an orbital liquid scenario<sup>35</sup> in the Mott insulating phase(s) in titanates.

In conclusion, using LSDA+DMFT, we study how orbital-selective charge dynamics in YTiO<sub>3</sub> is affected across the ferromagnetic-paramagnetic transition. The intricate orbital-dependent changes in optical response are understood as a direct consequence of the modification of the multiorbital, correlated electronic structure across  $T_C$ . Onset of magnetic order modifies the orbital occupations and hence the crystal-field splitting in the  $t_{2g}$  sector. In a strongly correlated system, these drive orbital-selective dynamical spectral weight transfer in response to these (small) modifications, resulting in the anisotropic changes in optical response across  $T_C$ .

L.C. and H.R. acknowledge support from the Emmy Noether-Programm of the DFG. M.S.L. thanks M. Grüninger for discussions and the MIPPKS, Dresden, for financial support. S.L. thanks the Swiss National Foundation for financial support. L.C. thanks E. Müller-Hartmann for discussions in early stages of this work.

- 
- <sup>1</sup>M. Imada, A. Fujimori, and Y. Tokura, *Rev. Mod. Phys.* **70**, 1039 (1998).
- <sup>2</sup>N. F. Mott, *Metal-Insulator Transitions* (Taylor & Francis, London, 1990).
- <sup>3</sup>S. Biermann, L. de' Medici, and A. Georges, *Phys. Rev. Lett.* **95**, 206401 (2005).
- <sup>4</sup>M. S. Laad, L. Craco, and E. Müller-Hartmann, *Phys. Rev. B* **73**, 045109 (2006).
- <sup>5</sup>J. P. Goral, J. E. Greedan, and D. A. Maclean, *J. Solid State Chem.* **43**, 244 (1982).
- <sup>6</sup>J. B. Goodenough, *Magnetism and the Chemical Bond* (John Wiley & Sons, New York, 1963).
- <sup>7</sup>A. B. Harris, T. Yildirim, A. Aharony, O. Entin-Wohlman, and I. Ya. Korenblit, *Phys. Rev. Lett.* **91**, 087206 (2003).
- <sup>8</sup>G. Khaliullin and S. Okamoto, *Phys. Rev. B* **68**, 205109 (2003).
- <sup>9</sup>H. Fujitani and S. Asano, *Phys. Rev. B* **51**, 2098 (1995).
- <sup>10</sup>J. Akimitsu, H. Ichikawa, N. Eguchi, T. Miyano, M. Nishi, and K. Kakurai, *J. Phys. Soc. Jpn.* **70**, 3475 (2001).
- <sup>11</sup>F. Iga, M. Tsubota, M. Sawada, H. B. Huang, S. Kura, M. Take-mura, K. Yaji, M. Nagira, A. Kimura, T. Jo, T. Takabatake, H. Namatame, and M. Taniguchi, *Phys. Rev. Lett.* **93**, 257207 (2004).
- <sup>12</sup>M. Mochizuki and M. Imada, *J. Phys. Soc. Jpn.* **70**, 1777 (2001).
- <sup>13</sup>R. Schmitz, O. Entin-Wohlman, A. Aharony, and E. Müller-Hartmann, *Ann. Phys.* **14**, 626 (2005).
- <sup>14</sup>E. Pavarini, S. Biermann, A. Poteryaev, A. I. Lichtenstein, A. Georges, and O. K. Andersen, *Phys. Rev. Lett.* **92**, 176403 (2004).
- <sup>15</sup>L. Craco, S. Leoni, and E. Müller-Hartmann, *Phys. Rev. B* **74**, 155128 (2006).
- <sup>16</sup>D. A. MacLean, H.-N. Ng, and J. E. Greedan, *J. Solid State Chem.* **30**, 35 (1979).
- <sup>17</sup>O. K. Andersen, *Phys. Rev. B* **12**, 3060 (1975).
- <sup>18</sup>G. Kotliar, S. Y. Savrasov, K. Haule, V. S. Oudovenko, O. Parcollet, and C. A. Marianetti, *Rev. Mod. Phys.* **78**, 865 (2006).
- <sup>19</sup>V. I. Anisimov, F. Aryasetiawan, and A. I. Lichtenstein, *J. Phys.: Condens. Matter* **9**, 767 (1997).
- <sup>20</sup>D. J. García, K. Hallberg, and M. J. Rozenberg, *Phys. Rev. Lett.* **93**, 246403 (2004).
- <sup>21</sup>A. Liebsch and T. A. Costi, *Eur. Phys. J. B* **51**, 523 (2006).
- <sup>22</sup>C. Ulrich, G. Khaliullin, S. Okamoto, M. Reehuis, A. Ivanov, H. He, Y. Taguchi, Y. Tokura, and B. Keimer, *Phys. Rev. Lett.* **89**, 167202 (2002).
- <sup>23</sup>M. B. Zöfl, Th. Maier, Th. Pruschke, and J. Keller, *Eur. Phys. J. B* **13**, 47 (2000).
- <sup>24</sup>R. Arita, K. Held, A. V. Lukoyanov, and V. I. Anisimov, *Phys. Rev. Lett.* **98**, 166402 (2007).
- <sup>25</sup>L. Craco, M. S. Laad, and E. Müller-Hartmann, *Phys. Rev. Lett.* **90**, 237203 (2003).
- <sup>26</sup>L. Craco, M. S. Laad, and E. Müller-Hartmann, *Phys. Rev. B* **68**, 233310 (2003); **74**, 064425 (2006).
- <sup>27</sup>M. S. Laad, L. Craco, and E. Müller-Hartmann, *Phys. Rev. Lett.* **91**, 156402 (2003).
- <sup>28</sup>A. Gössling, R. Schmitz, H. Roth, M. W. Haverkort, T. Lorenz, J. A. Mydosh, E. Müller-Hartmann, and M. Grüninger, arXiv:cond-mat/0608531 (unpublished).
- <sup>29</sup>R. Rückamp, E. Benckiser, M. W. Haverkort, H. Roth, T. Lorenz, A. Freimuth, L. Jongen, A. Möller, G. Meyer, P. Reutler, B. Büchner, A. Revcolevschi, S.-W. Cheong, C. Sekar, G. Krabbes, and M. Güninger, *New J. Phys.* **7**, 144 (2005).
- <sup>30</sup>A. Khurana, *Phys. Rev. Lett.* **64**, 1990 (1990).
- <sup>31</sup>E. Pavarini, A. Yamasaki, J. Nuss, and O. K. Andersen, *New J. Phys.* **7**, 188 (2005).

<sup>32</sup>L. Craco, C. I. Ventura, A. N. Yaresko, and E. Müller-Hartmann, Phys. Rev. B **73**, 094432 (2006).

<sup>33</sup>K. Tsutsui, W. Koshibae, and S. Maekawa, Phys. Rev. B **59**, 9729 (1999).

<sup>34</sup>L. Craco, M. S. Laad, S. Leoni, and E. Müller-Hartmann, Phys. Rev. B **70**, 195116 (2004).

<sup>35</sup>G. Khaliullin and S. Maekawa, Phys. Rev. Lett. **85**, 3950 (2000).